

openheart Assessment of stunned and viable myocardium using manganese-enhanced MRI

Nick B Spath ¹, Trisha Singh ¹, Giorgos Papanastasiou,¹ Andrew Baker,¹ Rob J Janiczek,² Gerry P McCann ³, Marc R Dweck ¹, Lucy Kershaw,¹ David E Newby,¹ Scott Semple¹

► Additional online supplemental material is published online only. To view, please visit the journal online (<http://dx.doi.org/10.1136/openhrt-2021-001646>).

To cite: Spath NB, Singh T, Papanastasiou G, *et al*. Assessment of stunned and viable myocardium using manganese-enhanced MRI. *Open Heart* 2021;**8**:e001646. doi:10.1136/openhrt-2021-001646

Received 10 March 2021
Accepted 14 May 2021



© Author(s) (or their employer(s)) 2021. Re-use permitted under CC BY-NC. No commercial re-use. See rights and permissions. Published by BMJ.

¹Centre for Cardiovascular Science, The University of Edinburgh, Edinburgh, UK

²GlaxoSmithKline Research and Development, Stevenage, UK

³Department of Cardiovascular Sciences, University of Leicester, Leicester, UK

Correspondence to

Dr Nick B Spath; Nick.Spath@ed.ac.uk

ABSTRACT

Objective In a proof-of-concept study, to quantify myocardial viability in patients with acute myocardial infarction using manganese-enhanced MRI (MEMRI), a measure of intracellular calcium handling.

Methods Healthy volunteers (n=20) and patients with ST-elevation myocardial infarction (n=20) underwent late gadolinium enhancement (LGE) using gadobutrol and MEMRI using manganese dipyridoxyl diphosphate. Patients were scanned ≤7 days after reperfusion and rescanned after 3 months. Differential manganese uptake was described using a two-compartment model.

Results After manganese administration, healthy control and remote non-infarcted myocardium showed a sustained 25% reduction in T1 values (mean reductions, 288±34 and 281±12 ms). Infarcted myocardium demonstrated less T1 shortening than healthy control or remote myocardium (1157±74 vs 859±36 and 835±28 ms; both p<0.0001) with intermediate T1 values (1007±31 ms) in peri-infarct regions. Compared with LGE, MEMRI was more sensitive in detecting dysfunctional myocardium (dysfunctional fraction 40.5±11.9 vs 34.9%±13.9%; p=0.02) and tracked more closely with abnormal wall motion (r²=0.72 vs 0.55; p<0.0001). Kinetic modelling showed reduced myocardial manganese influx between remote, peri-infarct and infarct regions, enabling absolute discrimination of infarcted myocardium. After 3 months, manganese uptake increased in peri-infarct regions (16.5±3.5 vs 22.8±3.5 mL/100 g/min, p<0.0001), but not the remote (23.3±2.8 vs 23.0±3.2 mL/100 g/min, p=0.8) or infarcted (11.5±3.7 vs 14.0±1.2 mL/100 g/min, p>0.1) myocardium.

Conclusions Through visualisation of intracellular calcium handling, MEMRI accurately differentiates infarcted, stunned and viable myocardium, and correlates with myocardial dysfunction better than LGE. MEMRI holds major promise in directly assessing myocardial viability, function and calcium handling across a range of cardiac diseases.

Trial registration numbers NCT03607669; EudraCT number 2016-003782-25.

INTRODUCTION

Coronary heart disease is a leading cause of morbidity and mortality worldwide^{1 2} and the subsequent development of heart failure

Key questions

What is already known about this subject?

► The ability to define viability following an acute myocardial infarction is invaluable in guiding management.

What does this study add?

► This study has demonstrated that manganese-enhanced MRI not only more accurately quantifies areas of myocardial dysfunction following ischaemic injury but can directly identify viable as well as recovering stunned myocardium.

How might this impact on clinical practice?

► We believe that manganese-enhanced imaging holds major promise for early detection and quantification of myocardial stunning and viability, with the potential for improved patient selection for revascularisation and novel therapeutic interventions for myocardial recovery.

is associated with major healthcare costs.³ Patients with ischaemic or dysfunctional myocardium benefit from pharmaceutical and revascularisation therapies⁴ but optimal patient selection is an ongoing and complex clinical challenge.

In MRI, late gadolinium enhancement (LGE) identifies areas of infarction and is an established measure of myocardial viability^{5 6} through its ability to define the scar burden and indirectly infer viability.⁷ However, accurate quantification of infarction in the acute setting can be challenging and infarct size is often overestimated, due to tissue oedema.^{8 9} ¹⁸F-fluorodeoxyglucose (¹⁸F-FDG) is a radio-labelled glucose analogue which is used in cardiac positron emission tomography (PET) to detect glucose metabolism in functional viable myocardium.¹⁰ This is considered gold standard for quantifying myocardial viability.^{11 12} However, its widespread use is limited by accessibility, radiation exposure and expertise. This highlights the lack

of alternative contrast media and our dependence on gadolinium-enhanced imaging.

Preclinical studies have demonstrated that manganese-enhanced MRI (MEMRI) accurately quantifies myocardial infarction, both at acute and chronic time points.^{13 14} Manganese, a calcium analogue, has comparable paramagnetic properties to gadolinium but is taken up by functional myocardium through cardiomyocyte calcium channels.¹⁵ Preclinical work has demonstrated excellent agreement between MEMRI and ¹⁸F-FDG PET in the quantification of myocardial viability.^{10 16 17} In this proof-of-concept study of patients with acute myocardial infarction, we aimed to assess the ability of MEMRI to discriminate viable from infarcted myocardium, to identify stunned but viable myocardium, and to provide a quantitative measure of myocardial calcium handling.

METHODS

This was a single-centre open-label observational cohort study.

Patients

Adult patients (≥18 years of age) with acute myocardial infarction were recruited from the Edinburgh Heart Centre between May 2018 and July 2019. Inclusion criteria were the diagnosis of ST-segment elevation myocardial infarction according to the universal definition of myocardial infarction¹⁸ and angiographically proven left main stem, left anterior descending or multivessel vessel disease. Patients were required to be clinically stable with reduced left ventricular ejection fraction (≤50% by echocardiography) secondary to one or more acute ischaemic events. Healthy volunteers were recruited as a control population and had no known pre-existing medical conditions. Exclusion criteria for all participants were any contraindication to MRI, contraindications to manganese dipyridoxyl diphosphate (MnDPDP) administration (high degree atrioventricular block, history of torsades de pointes or prolonged QTc interval, obstructive liver disease, maintenance on calcium-channel blockade or digoxin therapy), renal failure (estimated glomerular filtration rate <30 mL/min/1.73 m²), New York Heart Association class IV heart failure and women of child-bearing potential without a negative pregnancy test.

MRI

MRI was performed using a Siemens MAGNETOM Skyrafit 3T scanner (Siemens Healthineers, Erlangen, Germany), combining elements of spine and body array coils. All study participants underwent scanning with both LGE and MEMRI, 48 hours apart and in random order. Images were acquired with ECG-gating and during held expiration. Cine imaging was acquired with standard steady-state free precession sequences in long and short-axis orientations. T2 mapping was used to quantify T2, with T2 prepared steady-state free precession acquisition. T1 was quantified for each voxel using T1 mapping with Shortened Modified Look-Locker Inversion recovery

(ShMOLLI, WIP #1048 Siemens Healthineers).¹⁹ Quantitative estimation of native T1 was performed in a full short-axis stack from mitral valve annulus to apex and standard long-axis slices, with additional slices positioned appropriately to characterise pathology. T1 relaxation times were measured before and after administration of contrast media. After completion of the acute phase imaging protocol, patients were invited to return for repeat scanning with an identical protocol after 3 months (online supplemental methods).

Late gadolinium enhancement

LGE images were acquired from 7 min following intravenous administration of gadobutrol (0.1 mmol/kg; Gadovist, Bayer, Germany) using a single breath held phase-sensitive inversion recovery short-axis stack, and long axis orientations. A standardised inversion time of 400 ms was used and adjusted as required for optimal myocardial nulling. Postcontrast T1 mapping was performed with short-axis ShMOLLI stack 20 min after contrast administration (online supplemental methods).

Manganese-enhanced MRI

MEMRI was achieved using intravenous infusion of MnDPDP (5 µmol/kg, 1 mL/min; maximum dose of 10 mL/patient; Exova SL Pharma, Wilmington, Delaware, USA), imaging every 2.5 min following administration for 40 min, as described previously^{13 20} (online supplemental methods).

Image analysis

All analyses of T1 maps, LGE and cine-derived volumetric and functional sequences were performed using Circle Cardiovascular Imaging (CVI), CVI 42 V5.6.9, Calgary Canada, (online supplemental methods).

Kinetic modelling

To derive quantitative estimates and to assess differential manganese uptake, a compartmental model analysis was performed based on the Patlak formulation (online supplemental methods and figure S2).²¹ Contrast kinetic modelling was performed using in-house software²² developed in Matlab (MathWorks, V.R2016a, Natick, Massachusetts, USA).

Statistical analysis

All statistical analyses were performed with GraphPad Prism (GraphPad Software V.8.0.2, San Diego, California, USA). Continuous data were assessed for normality using the D'Agostino-Pearson test. Categorical baseline variables were compared using Fisher's exact test. To compare cardiac function and change in myocardial manganese uptake in patients and healthy volunteers, volumetric assessment and parametric mapping values were compared using paired or unpaired t-tests, Wilcoxon or Mann-Whitney tests, and analysis of variance (ANOVA) or Kruskal-Wallis tests as appropriate. Statistical significance was taken as two-sided $p < 0.05$.

Table 1 Baseline characteristics

	Healthy control subjects (n=20)	Patients with myocardial infarction (n=20)	P value
Male	13 (65)	16 (80)	0.5
Age	42±11	58±12	0.0003
BMI	26.0±2.9	28.0±4.3	0.1
Risk factors			
Hypertension	0	6 (30)	0.02
Smoking	0	10 (50)	0.0004
Dyslipidaemia	0	3 (15)	0.2
Diabetes mellitus	0	1 (5)	>0.9
Pre-existing IHD	0	4 (20)	0.1
Family history IHD	0	12 (60)	>0.0001
Infarct territory			
Infarct artery			
LAD		14 (70)	
RCA		4 (20)	
LCx		2 (10)	
PPCI to CMR (days)		3.2±1.8	

Values quoted are n (%) or mean±SD.

Bold values indicate statistical significance (<0.05).

BMI, body mass index; CMR, cardiac magnetic resonance; IHD, ischaemic heart disease; LAD, left anterior descending artery; LCx, left circumflex artery; PPCI, primary percutaneous coronary intervention; RCA, right coronary artery.

RESULTS

Twenty healthy volunteers and 20 patients following acute ST-segment elevation myocardial infarction underwent LGE and MEMRI scanning 48 hours apart. All patients were treated with primary percutaneous coronary intervention and underwent their first MRI at 3.2±1.8 days. The majority (n=13) of patients had peak high-sensitivity cardiac troponin I concentration >50 000 ng/L with the remaining seven patients having mean concentration of 36 621±13 574 ng/L (normal reference ranges: <34 ng/L for men and <16 ng/L for women). Fourteen patients agreed to return 3 months following myocardial infarction for repeat imaging with an identical protocol.

The patient group was older with more cardiovascular risk factors than healthy control subjects (table 1). Patients had lower ejection fraction and higher left ventricular mass index and extracellular volume fraction (p<0.0001 for all, table 2) with most presenting with anterior territory myocardial infarction (anterior, n=14, (70%); inferior, n=4, (20%), lateral, n=2 (10%)). Infarct size was similar between patients allocated to delayed-enhancement MRI or MEMRI first (35.2±12.9 vs 34.6%±15.6%, p=0.93).

Manganese infusion

Fifty-four infusions of MnDPDP were completed during the course of the study (mean duration 10 mins). There

were no changes in the ECG, heart rate or blood pressure (online supplemental figures S3 and S4) following MnDPDP administration (p>0.1 for all). One healthy volunteer experienced mild transient nausea for <10 s after commencing MnDPDP infusion, spontaneously resolving without intervention. Otherwise, administration of MnDPDP was well tolerated with no adverse reactions reported during or immediately after administration or at follow-up at 7 days.

MEMRI in healthy volunteers

In healthy volunteers, MnDPDP rapidly reduced blood pool T1 during the infusion (mean reduction 453±96 ms or 25.8%), followed by normalisation to baseline by 40 min (figure 1). Myocardial T1 also demonstrated a rapid initial descent (infusion phase) but this was followed by a slower, more gradual reduction which continued throughout the 40-minute imaging period (mean reduction 288±34 ms or 25.7%).

MEMRI in acute myocardial infarction

In patients with acute myocardial infarction, the T1 profile in areas of remote non-infarcted myocardium was similar to normal myocardium in the healthy volunteers (mean reduction 281±12 ms or 24.6%; compared with healthy volunteers, p=0.5). However, the T1 profile following MnDPDP in regions of myocardial infarction differed substantially. In particular, areas of transmural infarction demonstrated a partial recovery of T1 values similar to that of the profile observed in the blood pool (figure 2A,C), whereas in areas of less extensive subendocardial myocardial injury, T1 values plateaued after the infusion phase (figure 2B,D).

Across the entire cohort, MEMRI T1 values at 40 min were higher in regions of infarction compared with remote and healthy myocardium (1157±74 vs 859±36 and 835±28 ms; both p<0.0001). All infarct regions had MEMRI T1 >1000 ms, whereas remote and healthy myocardium had T1 <950 ms. An intermediate recovery profile and 40-minute MEMRI T1 value were demonstrated in peri-infarct regions (1007±31 ms), distinct from regions of infarction (1157±74 ms) and remote non-infarcted myocardium (859±36 ms; ANOVA p<0.0001, figure 3A).

Kinetic modelling of manganese uptake demonstrated stepwise reductions across remote, peri-infarct and infarcted myocardial regions, with absolute discrimination between the remote and infarcted myocardium (mean Ki 23.0±3.0, 16.7±3.8 and 11.7±3.5 mL/100 g/min; ANOVA p<0.0001, figure 3B). Rate of uptake between healthy control and remote non-infarcted myocardium was similar (23.1±3.6 and 23.0±3.0 mL/100 g/min; p=0.16), but uptake was slower in peri-infarct regions than remote myocardium (16.7±3.8 and 23.0±3.0 mL/100 g/min; p<0.0001).

Compared with LGE, MEMRI was more sensitive than LGE in detecting dysfunctional myocardium (dysfunctional fraction 40.5±11.9 vs infarct size 34.9%±13.9%; p=0.02) but these two measures of myocardial injury

Table 2 Cardiac magnetic resonance characteristics

	Healthy control subjects (n=20)	Patients with myocardial infarction (n=20)	P value	Patients with myocardial infarction and repeat imaging (n=14)		
				Acute	3 months	P value
Indexed EDV (mL/m ²)	74.7±14.4	86.2±19.1	0.04	83.2±16.2	87.1±16.1	0.3
Indexed ESV (mL/m ²)	26.8±7.3	46.7±16.0	<0.0001	44.8±13.8	41.6±12.1	0.2
Indexed SV (mL/m ²)	47.9±9.1	39.5±7.5	0.003	38.4±7.5	45.5±8.4	0.001
Ejection fraction (%)	64.4±5.5	46.7±8.8	<0.0001	46.9±8.9	52.9±7.9	0.0004
Mass index (g/m ²)	57.9±13.1	78.1±11.3	<0.0001	75.2±9.4	65.2±10.4	0.003
ECV (%)	27.1±3.6	37.9±2.5	<0.0001	37.0±1.9	36.7±3.5	0.9
Native T1 remote/healthy (ms)	1123±37	1143±44	0.1	1130±44	1110±41	0.2
MEMRI T1 remote/healthy (ms)	835±28	859±36	0.02	853±35	855±32	0.8
Infarct Characteristics						
Native T1 peri-infarct (ms)		1278±55		1278±56	1195±37	0.0005
Native T1 infarct (ms)		1395±73		1389±84	1295±71	0.002
MEMRI T1 peri-infarct (ms)		1007±31		1009±33	903±35	<0.0001
LGE (% LV)		30.3±10.2		30.5±9.6	19.3±7.3	<0.0001
Core Infarct Slice (%)						
LGE (FWHM)		34.9±13.9		35.1±12.5	24.2±6.5	0.005
T2 area-at-risk		47.1±11.0				
T1 area-at-risk		47.6±15.6		46.9±15.7	37.2±12.2	0.0004
MEMRI T1 injury		40.5±11.9		40.3±11.6	26.9±11.0	<0.0001
Influx constant (Ki, mL/100 g/min)						
Remote/healthy	23.1±3.6	23.0±3.0	0.2	23.3±2.8	23.0±3.2	0.8
Peri-infarct		16.7±3.8		16.5±3.5	22.8±3.5	<0.0001
Infarct		11.7±3.5		11.5±3.7	14.0±1.2	0.1

Values quoted are mean±SD or median±IQR.

Bold values indicate statistical significance (<0.05).

AAR, area at risk; ECV%, extracellular volume fraction; EDV, end-diastolic volume; EF, ejection fraction; ESV, end-systolic volume; FWHM, full width at half maximum; LGE, late gadolinium enhancement; MEMRI, manganese-enhanced MRI; SV, stroke volume.

correlated closely ($r^2=0.51$, $p=0.0004$). When compared with wall motion, MEMRI T1 tracked more closely with abnormal wall motion, demonstrating superior correlation than LGE (mean $r^2=0.72$ vs 0.55 , $p<0.0001$; [figure 4](#) and online supplemental figure S5).

MEMRI in recovery phase following myocardial infarction

In the cohort of patients (n=14) who underwent repeat imaging 3 months after myocardial infarction, average ejection fraction had increased by 6.0% ($p=0.0004$) and LGE infarct size had decreased by 11.2% ($p<0.0001$). At the core infarct slice, functionally impaired myocardium by MEMRI was on average 13.4% lower at 3 months than baseline ($p<0.0001$) and was similar to LGE quantification (26.9±11.0 and 24.2%±6.5%; $p=0.2$). Both native and MEMRI T1 in the remote non-infarcted myocardium remained unchanged between acute and recovery phase imaging (both $p>0.1$).

Using kinetic modelling, mean rate of manganese uptake was unchanged between early and late time points

in both infarcted (11.5±3.7 vs 14.0±1.2 mL/100 g/min, $p=0.1$) and remote non-infarcted (23.3±2.8 vs 23.0±3.2 mL/100 g/min, $p=0.8$) myocardium. In peri-infarct regions, the rate of manganese uptake was increased (16.5±3.5 vs 22.8±3.5 mL/100 g/min, $p<0.0001$; [figure 5](#) and [figure 6A,B](#)) suggesting recovery in myocyte calcium handling. In contrast to acute phase imaging, peri-infarct regions and remote myocardium demonstrated similar manganese uptake rates after 3 months (22.8±3.5 and 23.0±3.2 mL/100 g/min; $p=0.9$; [figure 6C](#)).

DISCUSSION

In this proof-of-concept study, we provide the first description of MEMRI T1 mapping to define viable and stunned myocardium in patients with acute myocardial infarction. Our study suggests that MEMRI can characterise and directly quantify viable myocardium, enabling it to be differentiated from infarcted and stunned myocardium. Furthermore, the kinetics of manganese uptake may

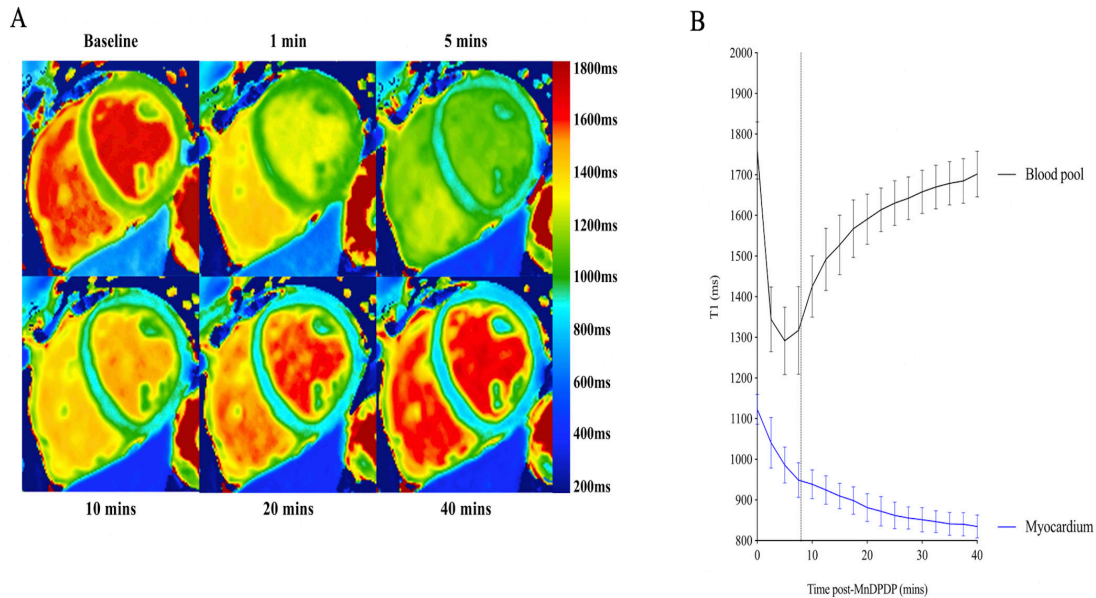


Figure 1 Manganese-enhanced MRI in healthy volunteers. Representative T1 colour maps (A) and T1 over time (B, n=20) following manganese dipyridoxyl diphosphate (MnDPDP). Dashed line represents mean end of infusion, SD of the mean.

provide a direct measure calcium handling within the myocardium. This latter property holds major promise for the future assessment of myocardial recovery as well as its potential application to other cardiac conditions associated with myocardial dysfunction and dysregulated calcium handling.

Manganese can be used to image tissues with calcium-dependent processes on account of its biophysical and kinetic properties as a paramagnetic calcium analogue.²³ Following intravenous administration of MnDPDP, rapid

biotransformation of the chelate occurs via dephosphorylation and transmetallation with zinc, enabling manganese to circulate as a bioavailable protein-bound complex that is readily accessible for intracellular uptake.^{23 24} Previous studies have demonstrated that manganese uptake is reduced in patients with ischaemic and non-ischaemic dilated cardiomyopathy.^{13 25} Furthermore, it correlates with left ventricular ejection fraction.²⁰

As anticipated, MEMRI detected clear differences in T1 values of the myocardium following acute infarction

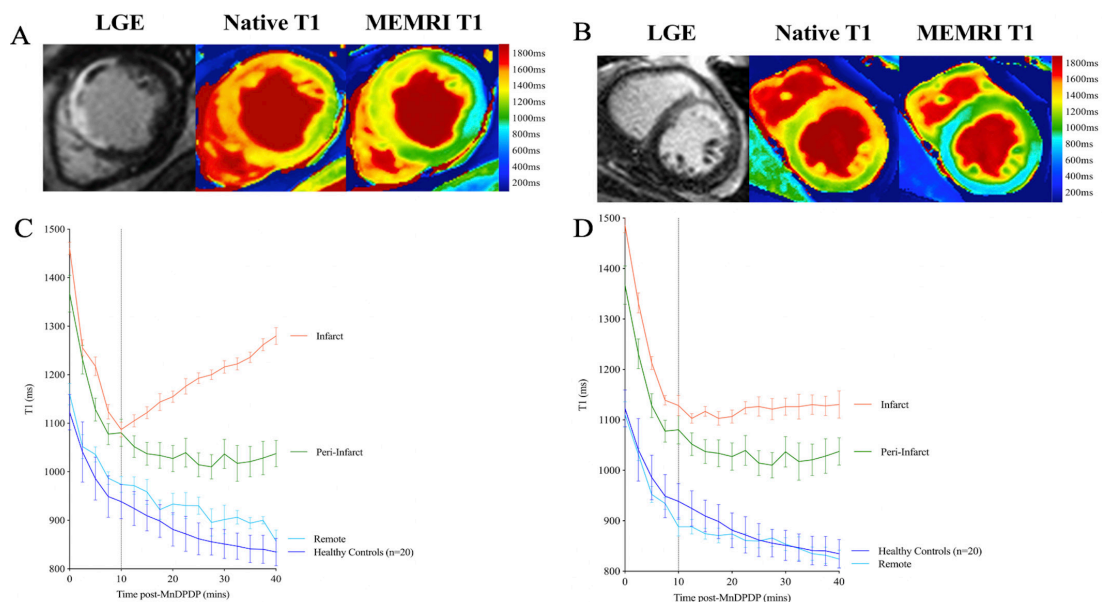


Figure 2 Manganese-enhanced MRI (MEMRI) in patients with myocardial infarction. Representative late gadolinium enhancement (LGE), native and MEMRI T1 mapping (A) and T1 profiles of myocardial regions of interest over time following manganese dipyridoxyl diphosphate (MnDPDP) (C) in a patient with extensive anterior myocardial infarction, compared with healthy control myocardium (n=20). Comparative representative LGE, native and MEMRI T1 mapping (B) and T1 profiles of myocardial regions of interest over time following MnDPDP (D) in a patient with subendocardial myocardial infarction, compared with healthy control myocardium (n=20). Dashed line represents end of infusion, error bars are SD of the mean.

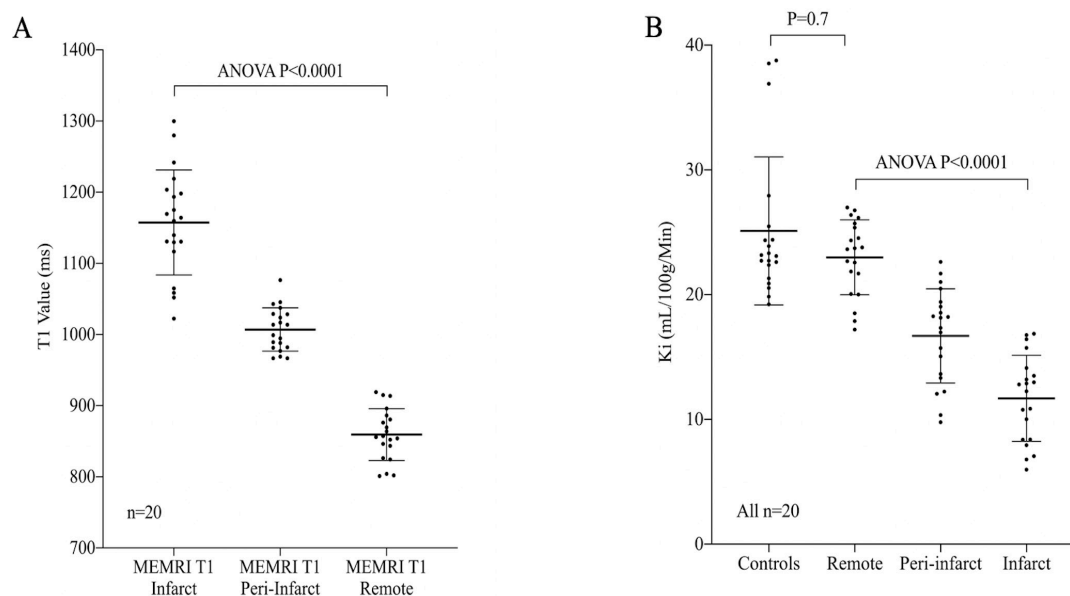


Figure 3 Manganese-enhanced MRI (MEMRI) in myocardial regions of interest. MEMRI T1 values in patients with myocardial infarction (A) and influx constant (Ki), (B) in patients with myocardial infarction; infarct core, peri-infarct and remote myocardial regions of interest, compared with healthy control myocardium. ANOVA, analysis of variance.

compared with peri-infarct and remote regions. Altered kinetics of manganese enhancement exceeded the region of infarction defined by LGE but correlated more closely with abnormalities in wall motion. This is an extremely important distinction as this suggests that MEMRI is more specifically tracking myocardial dysfunction where LGE only defines the pathological extracellular space

of infarcted or oedematous tissue. Furthermore, the changes in MEMRI T1 over 3 months after infarction may be attributable to alterations in calcium handling and uptake due to myocardial remodelling and recovery of cardiomyocyte function and contractility.

Within regions of extensive transmural myocardial infarction, the recovery of T1 values following infusion

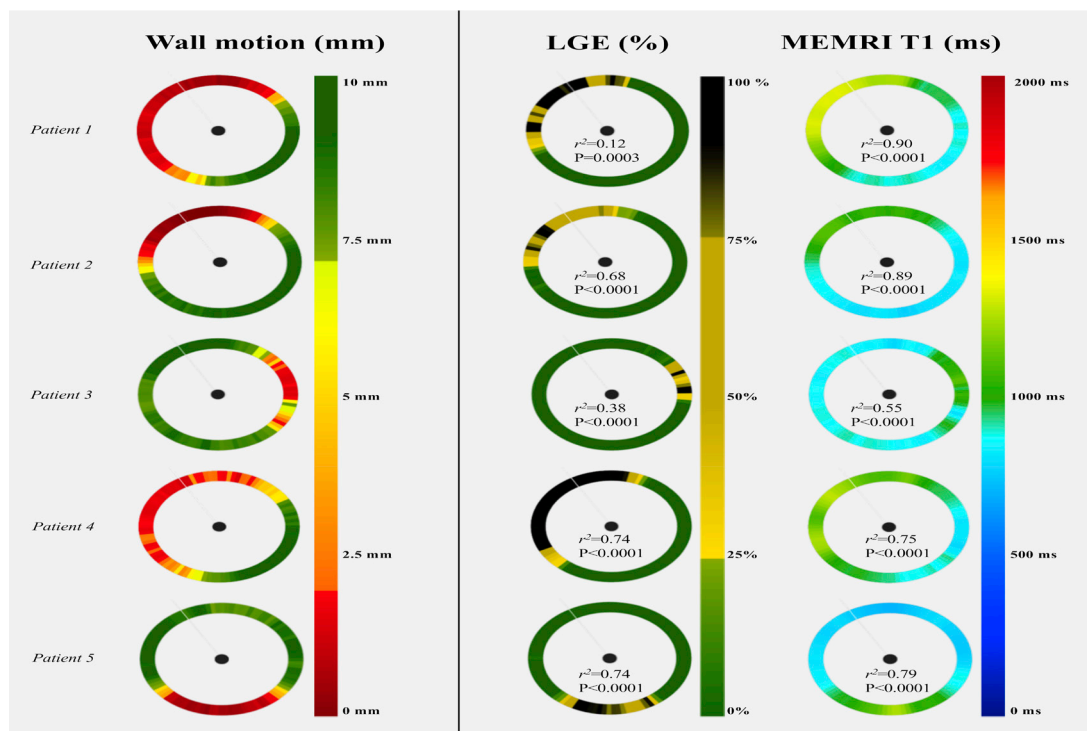


Figure 4 Wall motion, late gadolinium enhancement (LGE) and manganese-enhanced MRI (MEMRI) T1 mapping colour maps at the core infarct slice in five patients, represented as 100-chord plots (anterior right ventricle insertion as reference point). Values demonstrate stronger correlation between MEMRI T1 than LGE with reduced wall motion in every patient.

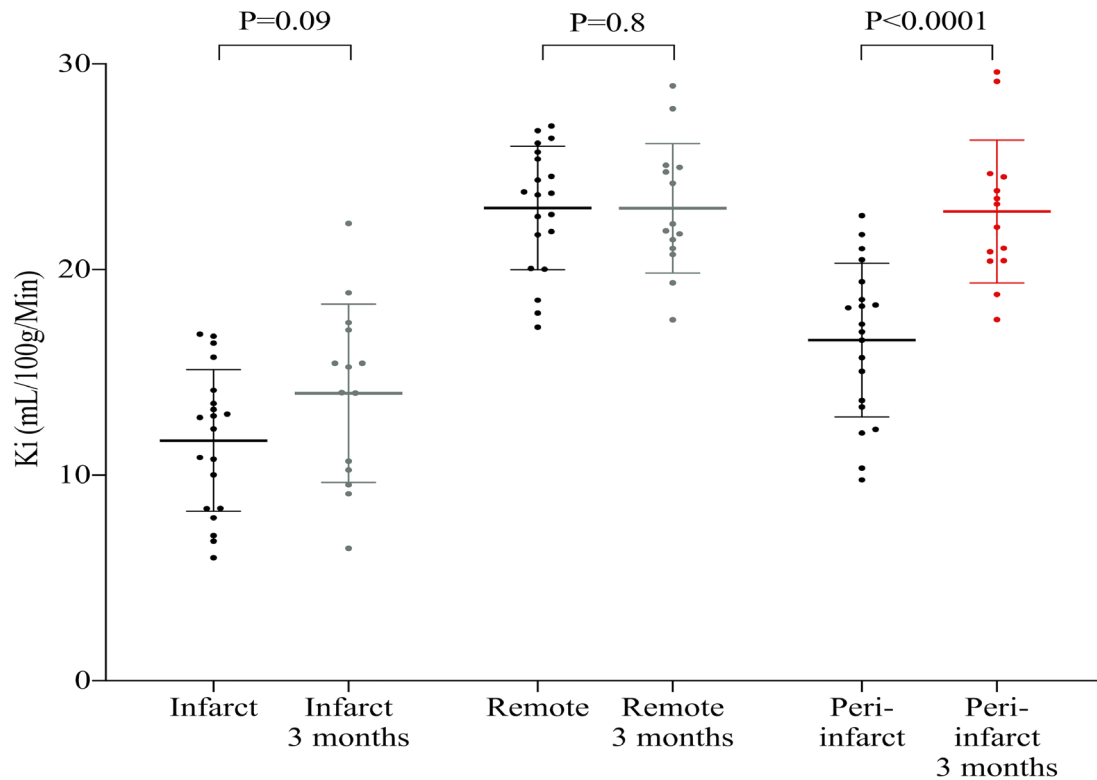


Figure 5 Differential manganese uptake over time. Kinetic modelling of manganese uptake (Ki, influx constant) in patients with myocardial infarction; infarct core, peri-infarct and remote myocardial regions of interest, at acute (n=20) and 3-month (n=14) imaging time points.

was similar to those seen in the blood pool. This recovery of T1 values suggests an absence of manganese uptake due to the presence of infarcted and non-viable tissue. The recovery of the T1 values was slower than the blood pool suggesting delayed clearance from the pathological extracellular space, similar to the mechanism by which gadolinium provides delayed enhancement. However, the plateau of T1 profile seen in patients with less extensive subendocardial myocardial infarction signifies that more complex contrast dynamics are at play. The plateau phase implies that some residual cardiomyocytes with viable calcium handling are present and is likely to represent a combined signal from both viable and non-viable cells within the wider infarct zone. Existing data suggest myocardial T1 shortening due to MnDPDP may persist several hours after administration²⁵ and therefore as a proof-of-concept study, it was important to image at later time points to yield better discrimination between myocardial regions according to functional impairment.

The extent of T1 shortening in the remote myocardium of patients with acute infarction was similar to that seen in healthy volunteers. This indicates there are no major alterations in remote myocardial calcium-channel handling detectable with MEMRI in the early stages following myocardial infarction. In contrast, peri-infarct regions demonstrated reduced rates of manganese uptake, indicative of reduced function in stunned but non-infarcted regions. Indeed, kinetic modelling demonstrated a stepwise reduction in calcium-channel activity

between remote, peri-infarct and infarct regions. Importantly, this reduction in manganese uptake in peri-infarct regions normalised after 3 months suggesting recovery of calcium handling by the stunned myocardium; a novel finding indicating MEMRI may be a sensitive tool in detecting myocardial viability. In this cohort of patients who underwent revascularisation for acute myocardial infarction, this ability to define viability by rate of calcium handling through the direct marker of manganese uptake could enable more accurate delineation of viable territories.

What are the clinical implications of MEMRI? In this study, we have undertaken the first T1 mapping investigation of MEMRI and have shown that it can identify viable myocardium and delineate it from infarcted as well as dysfunctional myocardium. Furthermore, for the first time, we have demonstrated that MEMRI can detect recovery of stunned myocardium within the peri-infarct zone following reperfusion. We, therefore, suggest that this technique has potential utility in detecting hibernating myocardium, which could prove an invaluable tool in patient selection for revascularisation therapies. Moreover, it holds particular promise as a biomarker of treatment efficacy for interventional strategies targeting ischaemia-reperfusion injury. With further study and optimisation of imaging time points, shorter imaging protocols will mean cardiac MEMRI assessment may offer a novel practical assessment of myocardial viability in clinical setting.

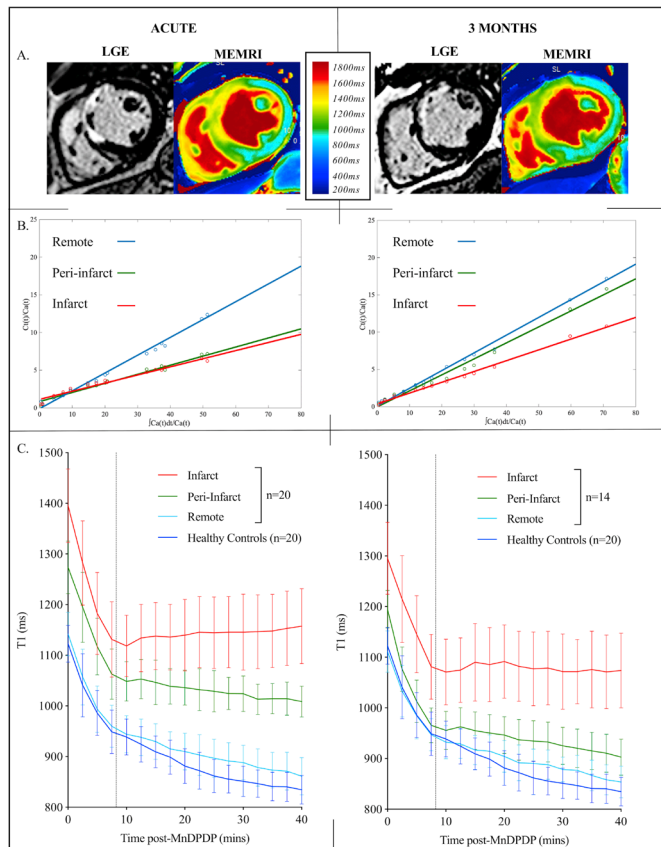


Figure 6 Differential manganese uptake after myocardial infarction. Representative late gadolinium enhancement (LGE) and manganese-enhanced MRI (MEMRI) T1 mapping images (A) and Patlak plots (B) in a patient with myocardial infarction, demonstrating differential K_1 (influx constant) between myocardial regions of interest over time. Grouped comparison T1 profiles for all patients and healthy control subjects (C). Dashed line represents end of infusion, error bars are SD of the mean. MnDPDP, manganese dipyridoxyl diphosphate.

Historically, there have been concerns that manganese-based contrast media could cause acute myocardial suppressant effects. Early animal studies used unchelated manganese chloride which caused negative inotropy and cardiovascular instability. In contrast, dipyridoxyl diphosphate chelates manganese and thereby markedly reduces free unbound manganese ions. To date, MnDPDP is the only manganese-based contrast agent which has been approved for clinical use as a liver-specific contrast agent.²² It was marketed as Teslascan but was removed from the US market in 2003²⁶ and subsequently from the European Union market in 2010²⁷ because it was not commercially viable. In the present study which included patients with acute myocardial infarction and the previous study by Skjold *et al*,^{16 20 25} MnDPDP was well tolerated in all subjects with no adverse events reported. This manganese-based contrast medium, therefore, appears safe and well tolerated. Given the resurgence of interest in this area, various companies are actively exploring re-marketing MnDPDP for clinical use.

Our study has some limitations. First, patients were recruited following primary percutaneous coronary intervention for acute myocardial infarction, which enabled the first evaluation of MEMRI in acute infarction. However, we did not exclusively recruit patients with single vessel disease or those with a first event. The presence of old infarction could have influenced the extent of recovery and our findings are therefore likely to be conservative. Second, LGE and MEMRI scans were performed 48 hours apart and, due to the dynamic nature of the infarct characteristics during the first week postrevascularisation, this may mean that the extent of contrast enhancement may have changed. To account for this, we randomised the order of scans which should eliminate any systematic bias in infarct size between LGE and MEMRI and measured oedema and LGE at the same time point in keeping with current consensus.⁷ A recent consensus suggested optimal imaging at 5 ± 2 days after myocardial infarction.²⁸ Due to the need to stagger MEMRI and LGE scans by 48 hours, we selected 3 ± 2 days in order to achieve this. Third, MnDPDP is currently not readily or widely available for clinical use although we anticipate that this is likely to change following the demonstration of its clinical and research utility. For the present study, we sourced a formulation of clinical grade MnDPDP. Fourth, our current MEMRI protocol lasts over 40 min which in a clinical setting may be challenging. However, this was a proof-of-concept study and we are currently exploring more rapid protocols to improve practical implementation. Fifth, we cannot rule out that calcium handling deteriorates with age and, because control subjects were younger, this could explain some of the observed reductions in manganese uptake. However, we found no correlation between age and manganese uptake in the healthy volunteers or our patient cohort (data not shown, $R^2=0.006$, $p=0.74$) and this would not explain the temporal changes in uptake seen in patients recovering from myocardial infarction. Finally, the small sample size of this pilot study warrants large scale translation.

In conclusion, we have described the first proof-of-concept T1 mapping study of MEMRI in healthy volunteers and patients with acute and recovering myocardial infarction. Using kinetic modelling, we have shown that MEMRI not only more accurately quantifies areas of myocardial dysfunction following ischaemic injury but can directly identify viable as well as recovering stunned myocardium. We believe that MEMRI holds major promise for early detection and quantification of myocardial stunning and viability, with the potential for improved patient selection for revascularisation and novel therapeutic interventions for myocardial recovery. Finally, its application to other areas of disorders of myocardial calcium handling warrants further investigation.

Acknowledgements Grateful acknowledgements are made to Siemens Healthineers for provision of the ShMOLLI WIP used in this study.

Contributors NBS, DEN and SS conceived and designed the study; NBS recruited and scanned all patients, analysed the data, performed kinetic modelling and compiled the original manuscript; GP wrote and validated the code for kinetic modelling; TS, DEN, GPM, MRD, AB, RJJ, LK and SS contributed to revision and critical appraisal of the final manuscript for important intellectual content. All authors approved the final manuscript submitted.

Funding This work and NBS, TS, AB, MRD and DEN are supported by the British Heart Foundation (FS/17/19/32641, FS/14/78/31020, CH/09/002, RG/16/10/32375, RE/18/5/34216, RG/20/5/34796). DEN is the recipient of a Wellcome Trust Senior Investigator Award (WT103782AIA). The Edinburgh Clinical Research Facilities and Edinburgh Imaging facility is supported by the National Health Service Research Scotland (NRS) through National Health Service Lothian Health Board.

Competing interests SIS has a consultancy agreement with GSK. DEN and SIS hold unrestricted educational grants from Siemens Healthineers.

Patient consent for publication Not required.

Ethics approval The study was carried out in accordance with the Declaration of Helsinki, the approval of the local Research Ethics Committee (17/SS/0055) and the written informed consent of all participants.

Provenance and peer review Not commissioned; externally peer reviewed.

Data availability statement All data relevant to the study are included in the article or uploaded as online supplemental information.

Open access This is an open access article distributed in accordance with the Creative Commons Attribution Non Commercial (CC BY-NC 4.0) license, which permits others to distribute, remix, adapt, build upon this work non-commercially, and license their derivative works on different terms, provided the original work is properly cited, appropriate credit is given, any changes made indicated, and the use is non-commercial. See: <http://creativecommons.org/licenses/by-nc/4.0/>.

ORCID iDs

Nick B Spath <http://orcid.org/0000-0001-9623-0158>

Trisha Singh <http://orcid.org/0000-0002-4314-9935>

Gerry P McCann <http://orcid.org/0000-0002-5542-8448>

Marc R Dweck <http://orcid.org/0000-0001-9847-5917>

REFERENCES

- Townsend N, Wilson L, Bhatnagar P, *et al.* Cardiovascular disease in Europe: epidemiological update 2016. *Eur Heart J* 2016;37:3232–45.
- Jernberg T, Hasvold P, Henriksson M, *et al.* Cardiovascular risk in post-myocardial infarction patients: nationwide real world data demonstrate the importance of a long-term perspective. *Eur Heart J* 2015;36:1163–70.
- Lesyuk W, Kriza C, Kolominsky-Rabas P. Cost-of-illness studies in heart failure: a systematic review 2004-2016. *BMC Cardiovasc Disord* 2018;18:74.
- Allman KC, Shaw LJ, Hachamovitch R, *et al.* Myocardial viability testing and impact of revascularization on prognosis in patients with coronary artery disease and left ventricular dysfunction: a meta-analysis. *J Am Coll Cardiol* 2002;39:1151–8.
- Anavekar NS, Chareonthaitawee P, Narula J, *et al.* Revascularization in Patients With Severe Left Ventricular Dysfunction: Is the Assessment of Viability Still Viable? *J Am Coll Cardiol* 2016;67:2874–87.
- Moon JC. What is late gadolinium enhancement in hypertrophic cardiomyopathy? *Rev Española Cardiol* 2007;60:1–4.
- Kim RJ, Wu E, Rafael A, *et al.* The use of contrast-enhanced magnetic resonance imaging to identify reversible myocardial dysfunction. *N Engl J Med* 2000;343:1445–53.
- Khan JN, Nazir SA, Singh A, *et al.* Relationship of myocardial strain and markers of myocardial injury to predict segmental recovery after acute ST-segment-elevation myocardial infarction. *Circ Cardiovasc Imaging* 2016;9:e003457.
- Kidambi A, Mather AN, Swoboda P, *et al.* Relationship between myocardial edema and regional myocardial function after reperfused acute myocardial infarction: an Mr imaging study. *Radiology* 2013;267:701–8.
- Beanlands RSB, Nichol G, Huszti E, *et al.* F-18-fluorodeoxyglucose positron emission tomography imaging-assisted management of patients with severe left ventricular dysfunction and suspected coronary disease: a randomized, controlled trial (PARR-2). *J Am Coll Cardiol* 2007;50:2002–12.
- Dilsizian V, Bacharach SL, Beanlands RS, *et al.* ASNC imaging guidelines/SNMMI procedure standard for positron emission tomography (PET) nuclear cardiology procedures. *J Nucl Cardiol* 2016;23:1187–226.
- Windecker S, Kolh P, *et al.*, Authors/Task Force members. 2014 ESC/EACTS Guidelines on myocardial revascularization: The Task Force on Myocardial Revascularization of the European Society of Cardiology (ESC) and the European Association for Cardio-Thoracic Surgery (EACTS) Developed with the special contribution of the European Association of Percutaneous Cardiovascular Interventions (EAPCI). *Eur Heart J* 2014;35:2541–619.
- Spath NB, Thompson G, Baker AH, *et al.* Manganese-enhanced MRI of the myocardium. *Heart* 2019;105:1695–700.
- Wen L-Y, Yang Z-G, Li Z-L, *et al.* Accurate identification of myocardial viability after myocardial infarction with novel manganese chelate-based MR imaging. *NMR Biomed* 2019;32:e4158.
- Massaad CA, Pautler RG. Manganese-enhanced magnetic resonance imaging (MEMRI). *Methods Mol Biol* 2011;711:145–74.
- Skjold A, Amundsen BH, Wiseth R, *et al.* MnDPDP as a viability marker in patients with myocardial infarction. *J Magn Reson Imaging* 2007;26:720–7.
- Spath N, Tavares A, Gray GA, *et al.* Manganese-enhanced T₁ mapping to quantify myocardial viability: validation with ¹⁸F-¹⁸F-fluorodeoxyglucose positron emission tomography. *Sci Rep* 2020;10:32029765.
- Thygesen K, Alpert JS, Jaffe AS, *et al.* Third universal definition of myocardial infarction. *Eur Heart J* 2012;33:2551–67.
- Piechnik SK, Ferreira VM, Dall'Armellina E, *et al.* Shortened modified look-locker inversion recovery (ShMOLL) for clinical myocardial T1-mapping at 1.5 and 3 T within a 9 heartbeat breathhold. *J Cardiovasc Magn Reson* 2010;12:69.
- Spath NB, Singh T, Papanastasiou G, *et al.* Manganese-enhanced magnetic resonance imaging in dilated cardiomyopathy and hypertrophic cardiomyopathy. *Eur Heart J Cardiovasc Imaging* 2020;00:1–10.
- Skjold A, Kristoffersen A, Vangberg TR, *et al.* An apparent unidirectional influx constant for manganese as a measure of myocardial calcium channel activity. *J Magn Reson Imaging* 2006;24:1047–55.
- Sutcliffe RP, Lewis D, Kane PA, *et al.* Manganese-enhanced MRI predicts the histological grade of hepatocellular carcinoma in potential surgical candidates. *Clin Radiol* 2011;66:237–43.
- Wang C, Gordon PB, Hustvedt SO, *et al.* MR imaging properties and pharmacokinetics of MnDPDP in healthy volunteers. *Acta Radiol* 1997;38:665–76.
- Du C, MacGowan GA, Farkas DL, *et al.* Calibration of the calcium dissociation constant of Rhod2 in the perfused mouse heart using manganese quenching. *Cell Calcium* 2001;29:217–27.
- Skjold A, Vangberg TR, Kristoffersen A, *et al.* Relaxation enhancing properties of MnDPDP in human myocardium. *J Magn Reson Imaging* 2004;20:948–52.
- Food and Drug Administration. Mangafodipir Trisodium
- European Medicines Agency. Teslascan (mangafodipir)
- Ibanez B, Aletras AH, Arai AE, *et al.* Cardiac MRI Endpoints in Myocardial Infarction Experimental and Clinical Trials: JACC Scientific Expert Panel. *J Am Coll Cardiol* 2019;74:238–56.